PROCEEDINGS OF SCIENCE

Jets and α_s Measurements at HERA

Artem Baghdasaryan*
DESY 22607 HAMBURG, YerPhI 375036 YEREVAN
E-mail: artem.baghdasaryan@desy.de

On behalf of the H1 and ZEUS collaborations

New results on normalised jet cross sections of inclusive, dijet and trijet production in DIS in the kinematic range of the exchanged boson (γ^*, Z^0) virtuality $150 < Q^2 < 15000\ GeV^2$ as well as inclusive jet production cross sections in the photoproduction regime ($Q^2 < 1\ GeV^2$) are presented. The measurements are used to determine the value of the strong coupling $\alpha_s(M_Z)$.

Photon 2013,
20-24 May 2013
Paris, France

*Speaker.

1. Introduction

The study of jet production in ep collisions at HERA has been well established as a testing ground of perturbative Quantum Chromodynamics (pQCD). While inclusive DIS gives only indirect information on the strong coupling via scaling violations of the proton structure functions, the production of jets allows a direct measurement of $\alpha_s(M_Z)$ and can further constrains the gluon density in parton distribution functions (PDFs). Due to presence of the resolve processes, jet production in photoproduction helps additionally to constrains the photon PDFs. Jet cross sections in NC DIS [1] and in photoproduction [2] are used as input for a pQCD analysis to extract the strong coupling $\alpha_s(M_Z)$.

2. Jet Production in Neutral Current DIS

The neutral current (NC) DIS data are measured with the H1 detector in bins of Q^2 and transverse jet momenta $P_{T,jet}$ for inclusive-jet and average transverse momenta $\langle P_{T,jet}\rangle$ for multi-jet events. The cross sections are normalised to the inclusive DIS cross section in the bins of Q^2. The normalised jet cross sections profit from smaller systematic experimental uncertainties compared to absolute jet cross sections. Furthermore the dependence on the Parton Distribution Function (PDF) chosen in the extraction of the strong coupling $\alpha_s(M_Z)$ from these measurements is reduced. The data are measured in the phase space with the exchanged vector boson (γ^*, Z^0) virtuality $150 < Q^2 < 15000 GeV^2$ and inelasticity $0.2 < y < 0.7$. The data were collected in 2005-2007 and correspond to an integrated luminosity of $\approx 300\text{pb}^{-1}$, which lead to a small statistical uncertainties even at large Q^2 and $P_{T,jet}$. Jets have been found in the Breit frame using inclusive k_T algorithm [5, 6]. To ensure that the jets are well contained within the acceptance of the calorimeter, an additional cut on jet pseudorapidities in the laboratory frame $-1.0 < \eta_{\text{Lab}} < 2.5$ are required. The inclusive-jet transverse momenta $P_{T,jet}$ is restricted to $7 < P_{T,jet} < 50\ GeV$ for inclusive-jet and to $5 < \langle P_{T,jet}\rangle < 50\ GeV$ for multi-jet events. The cross sections are measured simultaneously by performing a multi-dimensional unfolding [7]. The normalised inclusive-jet, dijet and trijet cross sections as a function Q^2, $P_{T,jet}$ and $\langle P_{T,jet}\rangle$ together with the NLO predictions are presented at figure 1. The QCD NLOJet++ [3] predictions give a good description of the data.

3. Jet Photoproduction

Single- and double-differential inclusive-jet cross sections in photoproduction are measured with the ZEUS detector for photon virtualities $Q^2 < 1\ GeV^2$ and γp centre-of-mass energies in the region $142 < W_{\gamma p} < 293\ GeV$. The data were collected in 2005-2007 and correspond to an integrated luminosity of 299.9 pb^{-1}. The jets are required to have $E_T^{jet} > 17$ GeV and $-1 < \eta^{jet} < 2.5$. The jets were reconstructed using either the k_T, the anti-k_T and the SIScone jet algorithms. The x region covered by the measurements was determined to be $0.003 < x < 0.95$. Two types of QCD processes contribute to jet production in photoproduction; the direct process, in which the photon interacts directly with a parton in the proton, and the resolved process, in which the photon acts as a source of partons, one of them interacts with a parton in the proton. The measurements of the inclusive-jet cross sections based on k_T algorithm are presented as functions of E_T^{jet} for

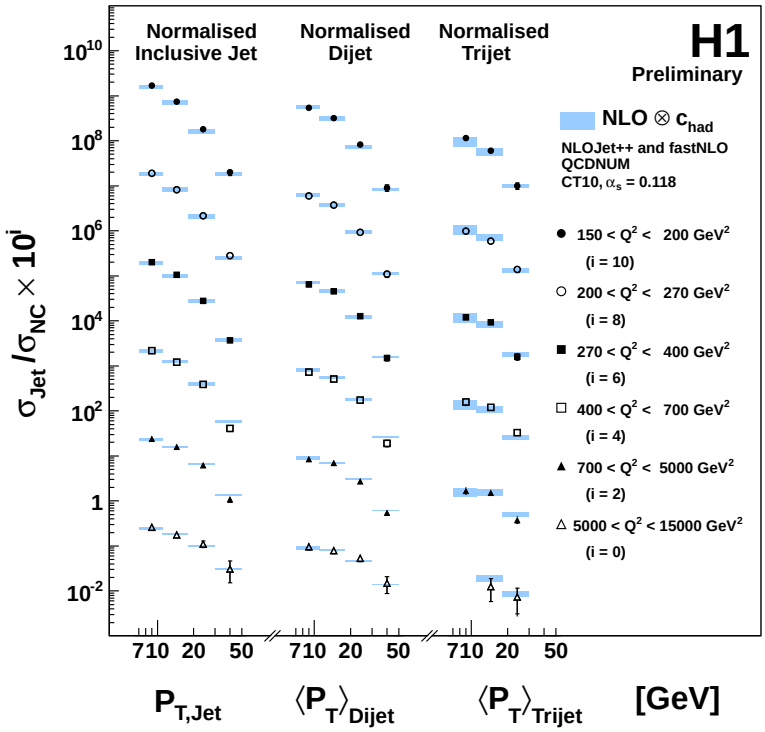

Figure 1: Normalised inclusive-jet, dijet and trijet cross section as functions of Q^2 and the transverse momentum in the Breit Frame $P_{T,jet}$. The inner error bars represent the statistical uncertainties. The NLO predictions are shown the symmetrised theory uncertainties determined by scale variations.

different regions of η^{jet} in figure 2. The NLO QCD predictions [8] give a good description of the data, except at low E_T^{jet} and high η^{jet}. These cross sections are sensitive to the parton densities in the proton and the photon in regions of phase space where theoretical uncertainties are small. The precision measurements presented here are therefore of particular relevance for improving the determination of the PDFs in future QCD fits. The ratios of measured cross sections $d\sigma/dE_T^{jet}$ and $d\sigma/d\eta^{jet}$ to the NLO QCD calculations are shown in figure 3 for three jet algorithms used. The measurements are well reproduced by the $O(\alpha_s(M_Z)^2)$ predictions, demonstrating the ability of the pQCD calculations including up to three partons in the final state to account adequately for the details of the differences between the SIScone and the k_T or anti-k_T jet algorithms. The measured cross sections were used to determine values of $\alpha_s(M_Z)$.

4. Extraction the Strong Coupling $\alpha_s(M_Z)$

Both measurements have been used to extract $\alpha_s(M_Z)$. A pQCD calculations, performed in next-to-leading order (NLO) of the strong coupling constant, have been fitted to DIS [9], [10] and photoproduction data [11]. The partons are grouped to jets using the same jet definition (k_T algorithm for NC DIS and k_T, anti-k_T and SISCone algorithms for photoproduction) as use for the

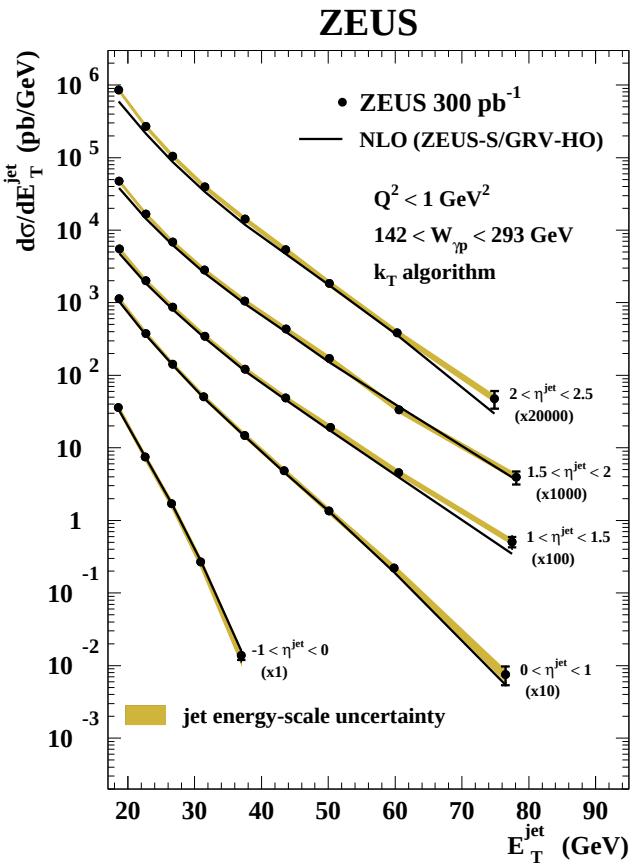

Figure 2: Measured differential cross-sections $d\sigma/dE_T^{jet}$ based on the k_T jet algorithm for inclusive-jet photoproduction with $E_T^{jet} > 17$ GeV in different regions of η^{jet} (dots) in the kinematic region given by $Q^2 < 1\ GeV^2$

data. For NC DIS data the strong coupling constant is determined from the normalised inclusive jet, dijet and trijet measurements as function of Q^2 and $P_{T,jet}$. To minimize the effects of possible non-perturbative contributions and to reduce higher orders uncertainties only multi-jets with $k < 1.3$ were using in the fit. Statistical correlations are considered in the fit throught the covariance matrix. The renormalisation scale is set to $\mu_r = \sqrt{(P_{T,jet}^2 + Q^2)/2}$, where $\langle P_{T,jet} \rangle$ is used instead of $P_{T,jet}$ for the dijet and trijet measurements. The factorisation scale is set to Q. The measured value of $\alpha_s(M_Z)$ is equal to:

$\alpha_s(M_Z) = 0.1163 \pm 0.0011(\text{exp}) \pm 0.0014(\text{pdf}) \pm 0.0008(\text{had}) \pm 0.0039(\text{theo})$.

For photoproduction data the strong coupling constant is determined from the single-differential cross sections $d\sigma/dE_T^{jet}$. To minimize the effects of a possible non-perturbative contribution coming from higher orders, only cross sections, measured in the range $E_T^{jet} > 21\ GeV$ were used to determine the values of the strong coupling constant. In addition, the fit was restricted to $E_T^{jet} < 71\ GeV$ to reduce the relatively large uncertainty coming from the proton PDFs. Measure value of $\alpha_s(M_Z)$ is equal to:

$\alpha_s(M_Z) = 0.1206 \pm 0.0023(\text{exp}) \pm 0.0042(\text{theo})$.

The values of $\alpha_s(M_Z)$, determined using the anti-k_T and SISCone algorithms, give almost identical

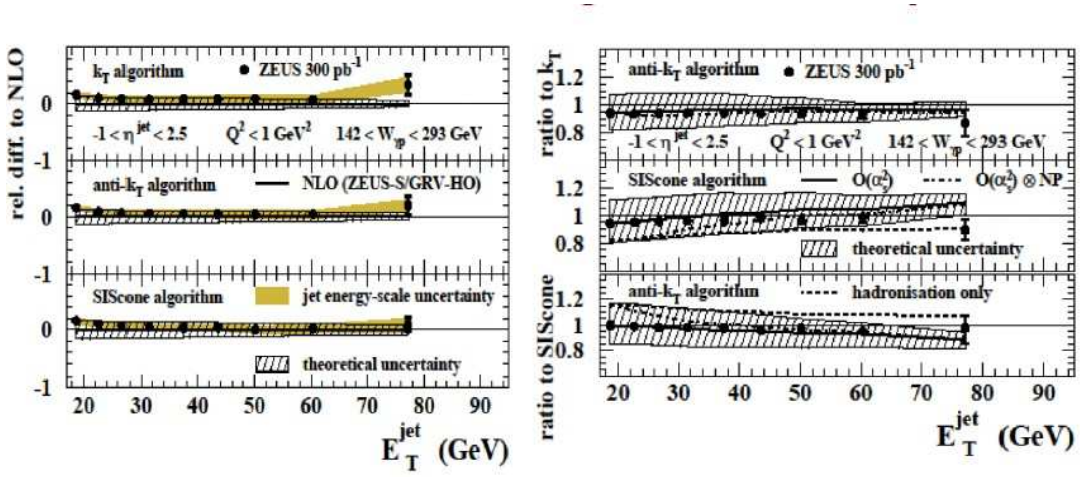

Figure 3: The relative difference to NLO predictions (left) and ratios of the measured cross sections anti-k_T /k_T, SIScone/k_T and anti-k_T /SIScone (dots) as functions of E_T^{jet}. In these plots, the outer error bars also include the uncertainty on the absolute energy scale of the jets. The predicted ratios are also shown (solid lines). The hatched bands display the theoretical uncertainty on the relative difference and ratio. The dashed lines indicate the ratios of the hadronisation correction factors and the dash-dotted lines represent the ratios of the NLO QCD calculations including an estimation of non-perturbative effects.

results.

The strong coupling constans determined from DIS and photoproduction data are consistent with each other and previously measured $\alpha_s(M_Z)$ and have a precision comparable to those, obtained from e^+e^- experiments. The total experimental uncertainties are considerably smaller than the theory uncertainties.

5. Summary

Measurements of normalised inclusive-jet, dijet and trjet cross sections in the Breit frame in NC DIS in the range $150 < Q^2 < 15000\ GeV^2$ and $0.2 < y < 0.7$ using the H1 detector as well as the measurements of differential cross sections for inclusive-jet photoproduction in the kinematic region of $Q^2 < 1\ GeV^2$ and $142 < W_{\gamma p} < 293\ GeV$ with three jet algorithms collected by the ZEUS detector have been presented. The NC DIS jet cross sections are simultaneously determined using a regularised unfolding procedure to correct for detector effect which takes into account all correlations among the data sets. NLO QCD calculations, corrected for hadronisation and Z boson exchange effects, provide a good description of the single and double differential cross sections as a function of the boson virtuality Q^2, the jet transverse momentum $P_{T,jet}$ in the whole phase space of the analysis. The NLO QCD calculations for photoproduction provide a good description of the measured cross sections, except at low $P_{T,jet}$ and high η^{jet}. Non-perturbative effects not related to hadronisation and the influence of the photon PDFs were found to be most significant in this region. A detailed comparison between the measurements for the three jet algorithms in photoproduction was performed. The values of $\alpha_s(M_Z)$ extracted from the jet cross sections in DIS and in γp. The uncertainties on the measurements of alphas from jet cross sections at HERA are dominated by the theoretical uncertainties because of missing NNLO calculations.

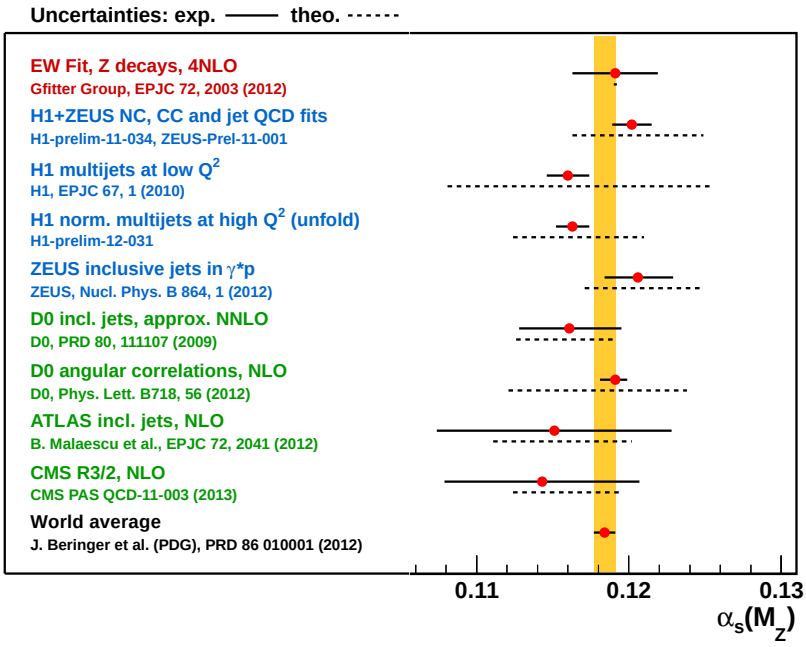

Figure 4: Extracted $\alpha_s(M_Z)$ value from the analyses presented here (the fourth and the fifth dots from up). For comparison, determinations from other experiments and reactions and the world average 2012 are also shown. The horizontal error bars represent the experimental (full line) and theoretical (dashed line) uncertainties. The shaded band represents the uncertainty of the world average

References

[1] *[H1 Collaboration] H1-Prelim-11-032, H1-Prelim-12-031*

[2] H. Abramovicz *et al. [ZEUS Collaboration], Nucl.Phys.* **B864** (2012) 1

[3] Z. Nagy and Z. Trocsanyi, *Phys. Rev. Lett.* **87** (2001) 82001

[4] S. Frixione and G. Rudolfi, *Nucl. Phys.* **B507** (1997) 315

[5] S.D. Ellis and D.E. Soper, *Phys Rev.* **D48** (1993) 3160

[6] S. Catani et al., *Nucl. Phys.*, **B, 406** (1993), 187

[7] S. Schmitt, *arXiv: 1205.6201*

[8] M. Klasen, T. Kleinwort, G. Kramer, *Eur. Phys. J.* **C1** (1998) 1

[9] J. Beringer et al., *Review of Particle Physics (RPP), Phys. Rev.* **D86** (2012) 010001

[10] V. Barone, C. Pascaud and F.Zomer, *Eur. Phys. J.* **C12** (2000) 243

[11] S. Chekanov *et al. [ZEUS Collaboration], Phys. Lett.* **B547** (2002) 164